



## Experimental Study on Compressive Behavior of Concrete-filled Double-skin Circular Tubes with Active Confinement

S. T. Nemati Aghamaleki<sup>a</sup>, M. Naghipour<sup>\*a</sup>, J. Vaseghi Amiri<sup>a</sup>, M. Nematzadeh<sup>b</sup>

<sup>a</sup> Department of Civil Engineering, Babol University of Technology, Babol, Iran

<sup>b</sup> Department of Civil Engineering, Faculty of Engineering and Technology, University of Mazandaran, Babolsar, Iran

### PAPER INFO

#### Paper history:

Received 10 November 2020

Received in revised form 23 December 2020

Accepted 04 January 2021

#### Keywords:

Concrete-filled Double-skin Tubes

Diameter-to-thickness Ratio

Active Confinement

Regression-based Design Formula

### ABSTRACT

A convenient family member of composite columns is concrete filled double skin tube (CFDST); it contains two tubes of concentric steel and also shell concrete that there is between them. The superior or equal potential offering characteristics of CFDST columns are more than counterparts of filled steel tubes of classical concrete (CFST). The purposes of the present study are to provide experimental investigation results into the prestressed load-carrying capacity of CFDST columns. Here, an innovative technique is used to confined concrete prestressing, in which the fresh concrete is compressed for a short-run duration. Sixty-four total specimens were tested with various outer thickness and diameter, inner thickness and diameter, and also CFDST columns of concrete strength that resist axial compression. The experimental results support that the present technique prestressed confined concrete, and it demonstrates that CFDST specimens' load-carrying capacity enhanced significantly.

doi: 10.5829/ije.2022.35.04a.22

## 1. INTRODUCTION

Provided confining pressure to the concrete core leads to deformability performance, ductility, and strength of reinforced concrete (RC) columns significant improvement; it can be done through the critical region and potential hinge of plastic. Most recently, transverse reinforcement of closely spaced installation is the most commonly adopted method to columns confining pressure improvement, which has been adopted in low-strength concrete columns made popularly [1, 2]. Therefore, confining steel content required for strength of higher concrete RC columns will dramatically enhance if the same ductility and strength level provided to the strength of lower concrete are constant [3, 4].

The design of columns can be as a member of composite to confining action efficiency improvement, in which confined of the concrete can be through FRP wraps [5, 6], steel plates [7, 8], and tubes of hollow steel [9-11]. The steel tube of concrete-filled (CFST) columns has

become popular in constructing tall buildings amongst these measures recently. One of the reasons is that CFST columns performance is superior to columns of ordinary RC under torsion [12, 13], under uni-axial load [14-18], and under flexure [19-21], based on experimental and theoretical research. Several examples of composite structures with CFST columns in circular or square forms, as external or internal structural members, are built. A good example in China is the Canton Tower in Guangzhou [1], comprising twenty-four inclined circular CFST members with a maximum diameter of 2000 mm and wall thickness of 50 mm. Another example is for Northern America. In the Museum of Flight at King County Airport (Seattle, Washington, USA) bar-reinforced concrete filled hollow sections are used for the columns supporting the roof of the exhibit hall, allowing to fulfil the required fire resistance without the need of sprayed fire protection [10]. Nevertheless, some disadvantages of CFST columns are as follows: (1) Under compression of uni-axial, steel can share the larger

\*Corresponding Author Institutional Email: [m-naghi@nit.ac.ir](mailto:m-naghi@nit.ac.ir)  
(M. Naghipour)

external load part's comparison concrete at the same area of cross-section because its stiffness is higher under the action of composite. (2) Under flexure, the contribution of central concrete, which is near the axis of neutral, to the strength of flexural is insignificant. (3) under torsion, the contribution of central concrete to the strength of torsion is insignificant. (4) the initial concrete elastic dilation under compression is fractional [22]. Therefore, the steel tube confining pressure to concrete during the stage of elastic is relatively low. The development of which can be more rapid until the formation of concrete micro-cracking at the immense strain [23]. The improvement on the CFST columns ratio of strength-to-weight is limited due to the infilled concrete heavy self-weight. The above discussions reveal that the in-filled concrete central part can replace another smaller tube of hollow steel with a similar strength of torsion, uni-axial, and flexure. This construction form of the column is known as the double skin tabular of concrete-filled (CFDST) columns [24].

Furthermore, Yagishita et al. [25] concluded that the absorption of energy, strength, and ductility of CFDST columns than CFT columns enhanced when they were subjected to axial loading and cyclic loading. Rahmani et al. [19] examined CFTs and CFDSTs cyclically and reached identical conclusions. Hence, the role of CFDSTs in the earthquake-affected becomes essential. The resistance of CFDSTs against fire is better than empty tubes and CFTs. Li et al. [26] deduced the existence of composite action among steel and concrete over fire exposure, and its fire performance is favorable.

Therefore, the deficiency of campaigns dealing with CFDST columns characterization and active confinement application study is prominent in the literature in this regard. Also, most of the tested CFDST columns had investigated the stiffness, ductility, and stiffness of SFDST with the pressure of passive confining. Active confinement is an innovative and novel avenue of studies and researches in this regard. The effectiveness of active confinement has increased by applying prestressing to material, where passive confinement depends on dilating concrete overloading to begin the confining pressures generation [27-29].

Typically, the confinement effect is expressed via the ratio of volumetric, which is the relation of reinforcement to the core of concrete. Thus, experimental program results evaluation is the main purpose of this study, where active confinement effects were compared and tested on tubes of double-skin circular concrete-filled in compression. The primary parameters of the ratio of diameter-to-thickness of the inner and outer tube, active confinement, and concrete compressive strength on load-carrying capacity were investigated to their effect on the general ductility and strength establishment. Finally, for the design purpose, a model of regression-base is proposed for the CFDST columns loading-carrying

capacity evaluation. The predicted strength of the results obtained by the authors and other researchers comparison regarding CFDST columns, validity of the proposed model was evaluated.

## 2. MATERIAL PROPERTIES

### 2.1. Steel Coupon Tests

With the aims of tensile coupons in order to grip were flattened through the test machine. The alignments of the coupons were carefully performed and accurately gripped. The incorrect alignment can cause the failure of premature due to the stresses of undesirable bending. The preparation and testing of the coupons were in the machine of displacement-controlled of 250 KN capacity (Figure 1). The test of the tensile coupon was conducted under the ASTM A370 [30] standard test with a 2 mm/min loading rate. The stress and strain were the computer's output data. These were plotted to establish the strength of ultimate, elasticity modulus, and yield strength. Table 1 demonstrates the summary of averaged material and individual properties. Where  $f_y$  indicates the strength of yield and  $f_u$  shows the strength of ultimate. Moreover, the averaged elastic modulus ( $E_s$ ) is reported as 200 GPa.



Figure 1. Shape of coupons for tensile tests

TABLE 1. Results of coupon test of circular hollow sections

Steel Coupon	$f_y$ (MPa)	$f_u$ (MPa)	$E_s$ (MPa)
SC1	345	410	$2.01 \times 10^5$
SC2	340	405	$2 \times 10^5$
SC3	350	420	$2.01 \times 10^5$
Average	345	411	$2 \times 10^5$

**2. 2. Concrete Cylinder Tests** As the final considered step in fabricating the experimental archetypes, the gap among the skins of hollow steel was suffused by Ordinary Portland Concrete (OPC). Two OPC grades (i.e., C10 and C20) were prepared in this study as the most commonly used mix is water, cement, and aggregates. Concrete specimens compressive strength were cast in the cylinder specimen of 150 (mm) × 300 (mm) and compacted based on ACI 211.1. Then, the cylinders were cured at the temperature of ambient. The results of the cylinder are summarized in Table 2.

### 3. TEST SPECIMENS

**3. 1. Specimen Preparation** Eight specimens' groups were tested with various values of  $D_i/t_i$ ,  $D_o / t_o$ , and  $f_c$  in this study. For each group, eight specimens were created, divided into the following categories containing two specimens: (1) prestressed compressed concrete of double-skin tube-confined; (2) non-prestresses concrete of double-skin tube-confined. Based on the definitions mentioned above, the confinement of prestressed compressed concrete of double-skin tube-confined is active. In contrast, the confinement of non-prestresses concrete of double-skin tube-confined is passive. Moreover, for only 15 to 30 min, the short-term pressure is applied to fresh concrete, that a stable pressure should be established during the process (Figure 2).

**TABLE 2.** Cylinder specimen for the properties of concrete

Concrete cylinders	Mass (g)	(MPa) $f_{cu}$	$E_c$ (MPa)
C10	2450	10	$1.48 \times 10^5$
C20	2450	20	$4.2 \times 10^5$



**Figure 2.** Applying preloading process on the fresh concrete

$$\sigma = E \times \varepsilon \quad (1)$$

where  $\sigma$  indicates stress,  $E$  represents elasticity modulus, and  $\varepsilon$  shows the strain.

$$\varepsilon = \frac{(0.5 \times 345)}{2 \times 10^5} = 860 \mu\varepsilon \quad (2)$$

So, it was decided to create two internal steel tubes types with diameters of 39mm and 1 mm thickness ( $t_i$ ) and 41mm with 2 mm thickness ( $t_i$ ). The selection of outer steel tubes was 114 mm ( $t_o = 2.5$ mm), 111.6 mm ( $t_o = 1.3$ mm), 8 mm 8 ( $t_o = 2$ mm), 86 mm ( $t_o = 1$ mm). The length of all columns was prepared at 250 mm. For fabricating sixty-four columns, 128 steel tubes were totally used to confirm the test results validity. The outer tube surface was shaved with the metal lathe to obtain various values for the thickness of the steel tube, while the steel tubes' inner diameter remained constant. Furthermore, metal lathes were cut off the specimens exceeded length after the active confinement to attain the genuine flat surface (see Figure 3).

The tubes tested dimensions are shown in Table 3, in which  $L_a$  indicates the column's actual length,  $D_o$  demonstrate the diameter of the outer tube,  $D_i$  shows the diameter of the inner tube. Besides,  $t_o$  and  $t_i$  represent the thickness of the outer and inner tubes. Figure 4 illustrates the composite columns' cross-section.

**3. 2. Concrete Cylinder Tests** Using the correlation of digital image (DIC), the CFDST columns' force-displacement values were recorded under the active or passive confinement. In order to obtain the displacement for the force applied per second, two points were signed at the end and top of the specimens based on this procedure (see Figure 5).

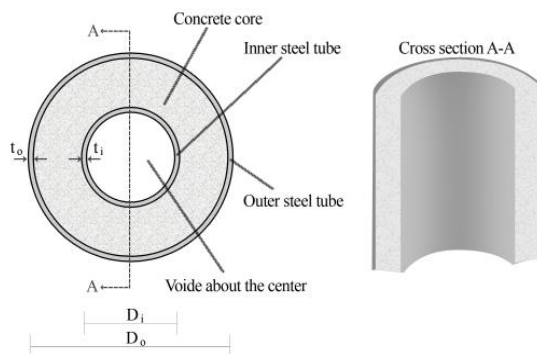
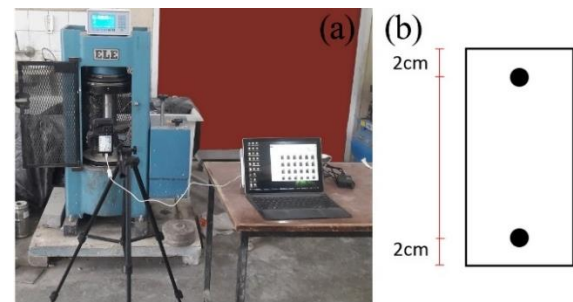
Using the testing machine of ELE with the capacity of 2000 kN after at least 28 days of curing time of the concreting date, these tests were accomplished. The amplification of load was based on the strategy of load-controlled until occurring the specimen failure. A load of



**Figure 3.** Before and after cutting off the process of a sample specimen

**TABLE 3.** columns' dimensional properties

Tag	$P_o$	$L_a/D_o$	$D_o/t_o$	$D_i/t_i$	$f'_c$ (MPa)
SN1-P	0	2.71	86	39	19.51
SN1-A	0.5 $f_y$	2.41	86	39	19.51
SN2-P	0	2.70	86	39	10.35
SN2-A	0.5 $f_y$	2.45	86	39	10.35
SN3-P	0	2.72	86	20.5	20.92
SN3-A	0.5 $f_y$	2.38	86	20.5	20.92
SN4-P	0	2.72	86	20.5	9.84
SN4-A	0.5 $f_y$	2.44	86	20.5	9.84
SN5-P	0	2.65	44	39	20.18
SN5-A	0.5 $f_y$	2.30	44	39	20.18
SN6-P	0	2.65	44	39	9.84
SN6-A	0.5 $f_y$	2.30	44	39	9.84
SN7-P	0	2.65	44	20.5	21.85
SN7-A	0.5 $f_y$	2.36	44	20.5	21.85
SN8-P	0	2.66	44	20.5	11.01
SN8-A	0.5 $f_y$	2.33	44	20.5	11.01
SN9-P	0	2.10	85.84	39	19.51
SN9-A	0.5 $f_y$	1.85	85.84	39	19.51
SN10-P	0	2.08	85.84	39	10.35
SN10-A	0.5 $f_y$	1.85	85.84	39	10.35
SN11-P	0	2.10	85.84	20.5	20.92
SN11-A	0.5 $f_y$	1.88	85.84	20.5	20.92
SN12-P	0	2.11	85.84	20.5	9.84
SN12-A	0.5 $f_y$	1.86	85.84	20.5	9.84
SN13-P	0	2.09	45.6	39	20.18
SN13-A	0.5 $f_y$	1.80	45.6	39	20.18
SN14-P	0	2.01	45.6	39	9.84
SN14-A	0.5 $f_y$	1.75	45.6	39	9.84
SN15-P	0	2.07	45.6	20.5	21.85
SN15-A	0.5 $f_y$	1.82	45.6	20.5	21.85
SN16-P	0	2.06	45.6	20.5	11.62
SN16-A	0.5 $f_y$	1.80	45.6	20.5	11.62

**Figure 4.** Composite column's cross-section**Figure 5.** a) DIC monitoring system; b) Schematic marking of the two points for force-displacement recoding of the specimens

axial with the average rate of a load equal to 42 kN/min was enhanced to 0.29 Mpa/s monotonically, which decreases within the 0.15 to 0.35 Mpa/s range that complies with the recommendations of ASTM C39 (ASTM C39/ C39M) [31] for concrete specimens.

## 4. RESULTS AND DISCUSSION









### 4. 1. Failure Modes

Since the ratios of diameter-to-thickness ( $D_o/t_o$  and  $D_i/t_i$ ), ratios of length-to-diameter ( $L_a/D_o$  and  $L_a/D_i$ ), and forces of active confinement were different, the steel hollow section's failure modes were different slightly under the axial compression. The local buckling by the portion of top to middle causes all of the CFDST specimens' failure modes observed to be under passive confinement. Nevertheless, local buckling was on the top specimens and specimens' end if the concrete was actively confined.

The attained CFDST specimen's failure modes were considered into the following groups: (1) the local buckling mode of the outer tube is subordinated with in-filled concrete shear failure. It is worth noting that which is similar to the CFDST columns' obtained results under passive confinement. (2) CFDST columns' local buckling mode under active confinement. Using filled concrete of C10 and C20, the investigation on one specimen failure mode was for outer tube diameter for 86 and 114 mm under the passive and active confinement (see Table 4). Figure 6 indicates the SN15 specimen's progressive failure under the active and passive confinement. The evident buckling of apparent steel was not observed in the points of (a) and (b) until attaining the first point of the peak. Nevertheless, point (c) deformation can be observed at the specimen's end with the axial load enhancement. Finally, in point (d), the buckling of outwards becomes apparent at the specimen's middle. All specimen of active confined processes (for instance, the points of (e), (f), and (g)) was identical to the passive. Point (h) was the exception of the local bulking area that experienced the buckling of outwards at the end and top specimen.



**TABLE 4.** CFDST columns' failure modes with the filled concrete of C10 and C20 under passive or active confinement

Type	Passive		Active	
	$D_o=86$	$D_o=114$	$D_o=86$	$D_o=114$
C10				
C20				

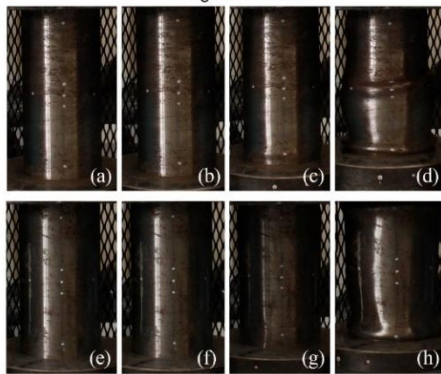
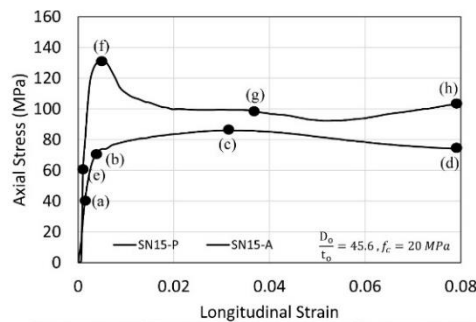


**Figure 6.** Failure modes of SN15 specimen under passive and active confinement

**4. 2. Specimens' Comparison under Active/Passive Confinements**

Figures 7 and 8 illustrate the stress of axial is plotted toward the strain that obtained for tubular columns of concrete-filled of double-skin (CDFST) without and with the active confinement ( $0.5f_y$ ), also with different  $D_i(39t_i, 20.5t_i)$ , and  $D_o(86t_o, 84t_o, 45.6t_o, 44t_o)$ . The curves of the present study represent axial deformation with the strain of nominal axial that measured as the deformation of general axial ratio to the initial length of the column. CFDST columns' steel skin in the condition of passive buckled severely, and deformations of the plastic enhanced rapidly at the

specimens' middle by achieving the strength of the ultimate specimen. Nevertheless, occurring the ultimate

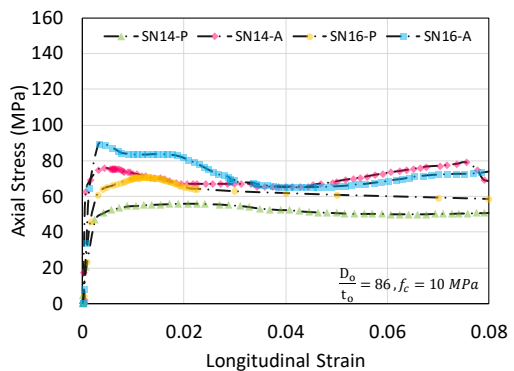
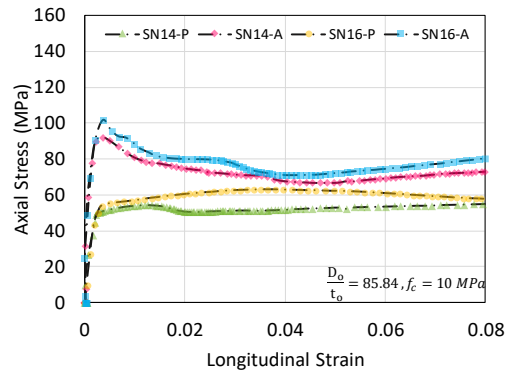
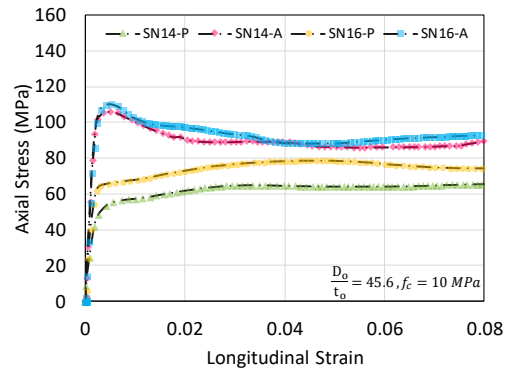
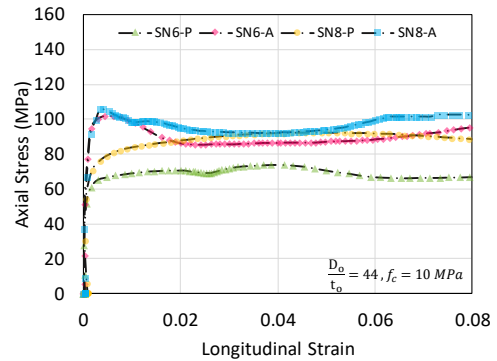


**Figure 7.** Strain-stress curve under active confinement against passive confinement for C10 filled concret

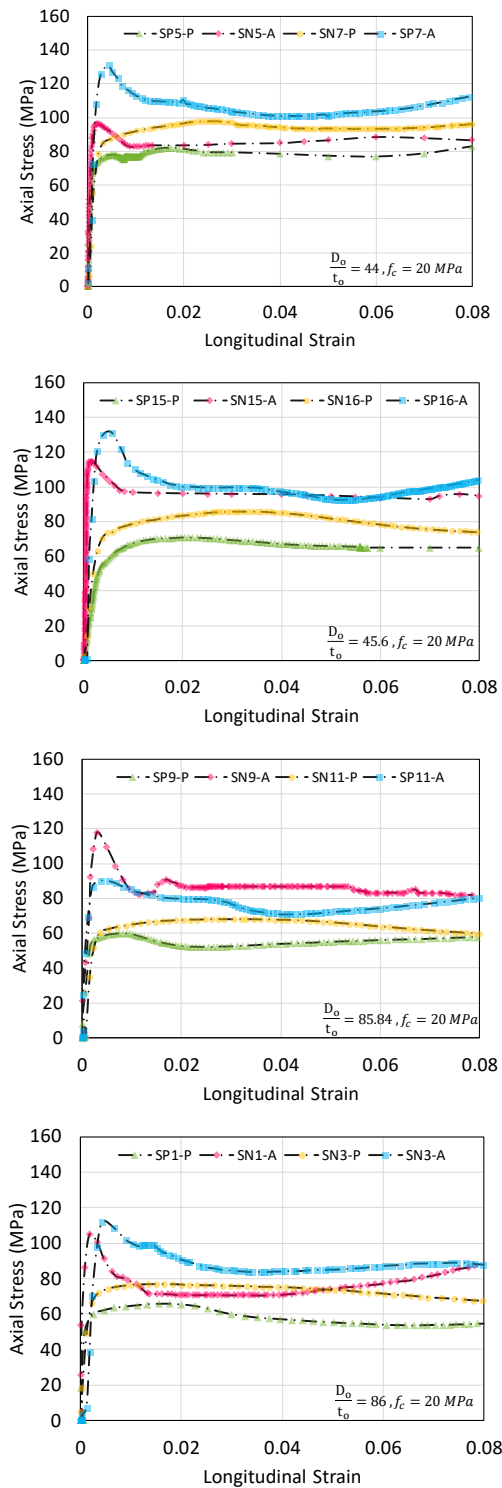


**Figure 8.** Strain-stress curve under active confinement against passive confinement for C20 filled concrete

strength, deformations at the specimens' end and top increase under the active preloading. This phenomenon causes a drop of abrupt in the curve of stress-strain

simultaneous to infill concrete crushing. The loading procedure was concluded since the experiment's progress became very slow after the peak load by dropping specimen capacity for filled concrete of C10 and C20 under the active confinement.

Figures 7 and 8 noticed that the drop of axial stress after the terminal load under the passive confining was not abruptly against the longitudinal strain curves. Instead, it was processed by the long ductility stage. The good performance of ductility exhibits by the results of the tested specimens. Moreover, the CFDST stress axial compressive for columns of filled concrete of C10 and C20 under the condition active preloading decreased as the ratio of  $D_o/t_o$  was enhanced, as indicated in the figures. For instance, the CFDST specimens' ultimate strength with filled concrete of C10 decreased to 15% approximately when the ratio of  $D_o/t_o$  amplify from 44 to 86. For the filled concrete of C20, increasing the  $D_o/t_o$  ratio from 44 to 86 experienced a 12% reduction.

Degradation in the specimens' ductility and compression capacity could be imputed to the inner or outer tubes' characteristics according to the curves of stress-strain for filled concrete of C10 and C20. The external tube's ratio of  $D_o/t_o$  is higher ( $D_o/t_o = 86$ ). So, due to the early buckling of local outward, it suffers, and outer steel section compression capacity cannot efficiently be exploited. The thicker external steel tube of CFDST specimens (SN7-A and SN8-A) development has a greater compression capacity over the SN4-A and SN3-A specimens. Results confirm the effect of active confinement on the circular tube of a double skin. Filled concrete of C20 has better performance than its load of crushing since the standard strength concrete of C10 in the specimens of CFDST is appropriately confined. Moreover, the outcomes of this study imply that the  $D_i/D_o$  affects the strength of ultimate axial of short circular columns of CFDST roughly subject to the condition of preloading. The strength of axial compressive columns for the circular columns of CFDST that are short with  $D_i/t_i$  equivalent to 20.5 (the range of  $D_i/D_o$  was from 0.36-0.48) enhanced by decreasing  $D_i/D_o$ .

#### 4. 3. Different Inner Diameter's Effect on the Ratios of Thickness under the Active/Passive Confinements

Figures 9 and 10 were depicted based on the characteristics of the internal tube effect subject to active or passive confinement for the filled concrete of C10 and C20 in columns of CFDST, respectively. As results show, axial loading capacity is enhanced gradually by  $D_i/t_i$  reduction for filled concrete of C10 and C20 subject to active or passive confinement. For example, since the ratio of internal diameter to thickness for  $D_o/t_o = 86$  enhanced from 25.5 till 39, axial loading capacity for C20 and C10 subject to active confinement reduced by 26% and 14.28%, respectively. It is noteworthy that for  $D_o/t_o = 44$ , this decreased for

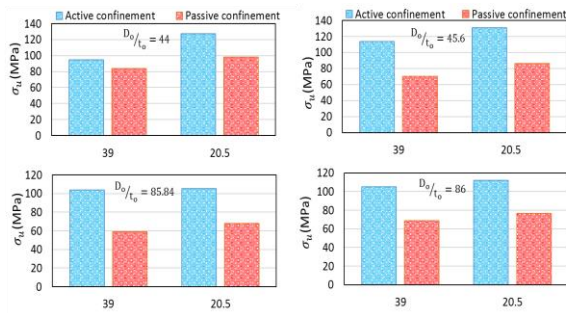


**Figure 9.** Compressive stress of CFDST specimens under passive and active confinements for C10 concrete

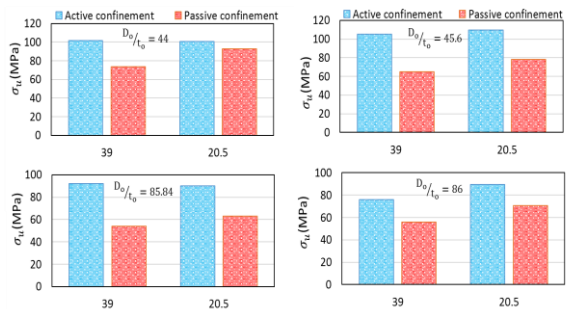


**Figure 10.** Compressive stress of CFDST specimens under passive and active confinements for C20 concrete

active confinement was approximately 2.19%. Additionally, when using filled concrete of C10, it was reported that passive confinement reduced axial loading capacity by around 22% compared with active confinement. Furthermore, if the  $D_o/t_o$  was constant, the axial loading capacity associated with reducing the thickness tube or internal diameter could not increase specifically. Therefore, the lower  $D_i/t_i$  for columns of CFDST can be used subject to the condition of active preloading.

Improving the strength of CFDST specimens axial compressive can be occurred by the outer steel tube's strength of concrete and ratio of diameter to thickness subject to active confinement. Consequently, the effect of active confinement on CFDST specimens, in addition to inner and outer steel tubes' contribution to columns' ultimate compression load in such significant enhancement, is essential.

#### 4. 4. Prediction Of CFDST Column Strength

In order to predict the capacities of members bearing, structural design is highly essential. A consistent sensitivity and reliability framework must spread realistic and accurate approaches of prediction if failure is avoided. Thus, the design of the specifications step is done with the aim of standard methods, and the prediction of offer capacity is formulated based on various theories' backgrounds. The most prominent

design specifications of composite members are the ACI code [33] associated with some tentative equations provided by Hassanein et al. [34] and Uenaka et al., [35] which are widely used for research aims. Today, the technology of composite members is constantly evolving, and compression's new form is created sections arise. Hence, the development of other technical approaches is compulsory to satisfy composite construction's needs. In this line, considering the active preloading to prediction capabilities assessment, this section of the study suggested a novel formulation for columns of a double skin. A fundamental understanding of methods and also underlying theories is essential before comparing results .

1) By the equation obtained using the ACI code [32], the strength of the ultimate axial of composite columns of single skin containing the bar of reinforcing can be determined. Nevertheless, with the ACI code [32], the effect of concrete confinement on the proposed formula is ignored. The following modified equation that obtained from the ACI code [32] is for the strength of the CFDST stub column ultimate axial involving internal steel tube contribution is declared as follows:

$$(P_u)_{ACI} = f_{yo}A_o + 0.85f_cA_c + f_{yi}A_i \quad (3)$$

Where  $f_{yo}$  and  $f_{yi}$  indicate the strength of yield of outer and internal steel tubes, respectively. Besides,  $f_c$  demonstrate the strength of compressive of annulus concrete.  $A_o$  and  $A_i$  show the area of cross-sectional of the outer and internal steel tubes, respectively. Finally,  $A_c$  represents the area of cross-sectional of annulus concrete.

2) Additionally, some researchers suggested equations for the strength of the CFDST columns ultimate axial's calculation in order to modify the ACI code recommended formula. Uenaka et al. [33] obtained the determining equation of strength of CFDST columns ultimate axial from the proposed equation of Architectural Institute of Japan (AIJ) [34] for the columns of CFST stub. The strength of sandwiched concrete and inner and outer steel tubes is superimposed elementally by Uenaka et al. [33]. Next, the effect of confinement of the inner tube on the strength of CFDST columns ultimate axial is not as practical as the outer one [1]. Uenaka et al. [33] followed modified expression of ultimate axial strength estimation is obtained from AIJ [34]:

$$(P_u)_{Uenaka \ et \ al.} = (2.86 - 2.59\left(\frac{D_i}{D_o}\right))f_{yo}A_o + 0.85f_cA_c + f_{yi}A_i, \ for \ 0.2 < \left(\frac{D_i}{D_o}\right) < 0.7 \quad (4)$$

where the internal steel tubes diameter is shown by  $D_i$ . 3) the proposed model of Hassanein et al. [35] could be used to strengthen the ultimate axial of circular stub columns of CFDST, and that estimates the strength of the ultimate axial of circular stub columns of CFST. It is

noteworthy that it is based on the design model, and Liang and Fragomeni's [36] developed it regarding the previous model proposed by Hassanein et al. [35]. It aims to predict the strength of the ultimate axial of stub columns of CFDST involving carbon steels and stainless. The following model of novel design is extended by Hassanein et al. [35]:

$$(P_u)_{Hassanein et al.} = \gamma_o f_{y_o} A_o + (\gamma_c f_c + 4.1 f'_{rp,o}) A_c + \gamma_i f_{y_i} A_i \tag{5}$$

where the coefficient of  $\gamma_o$  can be used for the effect of strain hardening explanation on the external steel, and it can obtain as follows:

$$\gamma_o = 1.458 \left(\frac{D_o}{t_o}\right)^{-0.1}, \quad 0.9 < \gamma_o < 1.1 \tag{6}$$

$\gamma_c$  shows the recommended strength attenuation coefficient of Liang [37], and also can obtain as follows ( $D_c$  means  $D_o - 2t_o$ ):

$$\gamma_c = 1.85 D_c^{-0.135}, \quad 0.85 < \gamma_c < 1.0 \tag{7}$$

The pressure of lateral confining of  $f'_{rp,o}$  for  $47 < \frac{D_o}{t_o} < 150$  expressed as follows:

$$f'_{rp,o} = (0.006241 - 0.0000357 \frac{D_o}{t_o}) f_{y_o} \tag{8}$$

The coefficient of  $\gamma_i$  can explain the effect of strain hardening on the internal steel and can be obtained as follows:

$$\gamma_i = 1.458 \left(\frac{D_i}{t_i}\right)^{-0.1}, \quad 0.9 < \gamma_i < 1.1 \tag{9}$$

Based on the study's results, the main parameter that affects the final stress in the tubes of a double skin of filled concrete is the factor of active confinement. In the present study, the analysis of multi-expression linear regression was applied to present a comprehensive and novel relationship that can use for the active and passive confinement in the columns of CFDST. The following formula is extracted from the linear regression of multi-expression:

$$(P_u)_{Present study} = 303.54A - 147.81 \frac{L_a}{D_o} + 3.934 \frac{D_o}{t_o} - 3.1 \frac{D_i}{t_i} + 8.163 f_c + 0.762 A_{so} + 12082.82 \left( (0.006241 - 0.0000357 \frac{D_o}{t_o}) f_{y_o} \right) - 25266.9 \tag{10}$$

The effective coefficient is shown by A subject to active confinement and considered 0 and 0.5 for passive and active confinement.

Figure 11 indicates the test results of CFDST specimens' predicted scatter plots and values of observed  $P_u$ . The data reported by others as shown in Figure 11 are scattered with low  $R^2$ . However, our data are close to the linear model with high  $R^2$  value of 0.89. In Figure 11, almost all values of predicted  $P_u$  from Hassanein et al. [35] and ACI code [32] were underestimated. Nevertheless, the present study and Uenaka et al. [33] predicted  $P_u$  are closer to an ideal line ( $y=x$ ). The  $R^2 =$

0.61 obtained from the Uenaka et al. [33] proposed method is better among the three empirical methods.

It is worth noting that none of the three methods consider the effect of active confinement. It is possible to adapt a novel method to composite the processes of column design with high-fidelity and accurate modifications that include active confinement. Figure 12 exhibits the relevance presented equation and traditional methods error to implement the prediction error outcomes visually.

Table 5 shows the empirical equation comparison and the proposed equation of regression-baes according to the strength values of normalized ultimate axial. The predicted capacities of axial load-carrying for the columns of CFDST are not accurate almost because the tentative equations do not consider the active confinement effect. The performance of the Uenaka et al. [33] proposed method with the average ratio 1.02 and 0.23 standard deviation is better among the three

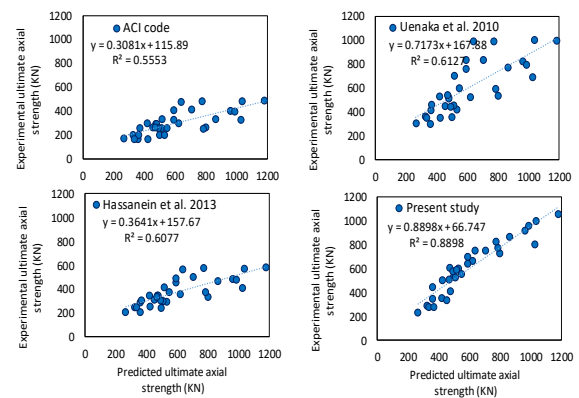


Figure 11. Scatter plots between the observed and the predicted value of  $P_u$  for the proposed and existing equations

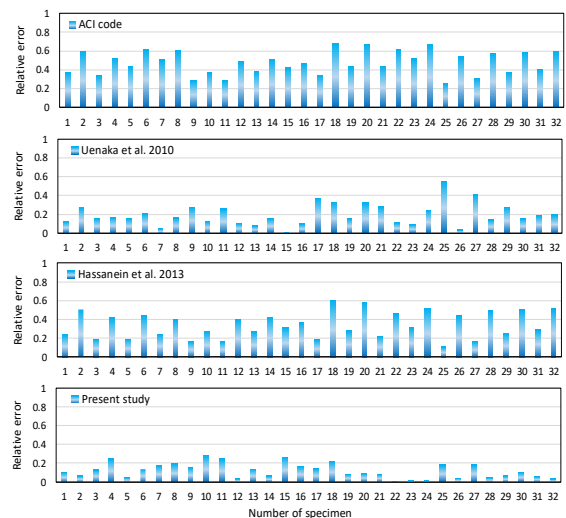


Figure 12. Relative error plots of the proposed and existing equations for the ultimate axial strength of CFDST columns



**TABLE 5.** Comparison of the experimental ultimate axial strength of CFDST columns with and without active confinement for the proposed and existing equations

$N_u$ (KN)	$N_u/N_{u-ACI}$	$N_u/N_{u-Uenaka}$	$N_u/N_{u-Hassanein}$	$N_u/N_{u-MLR}$
324.74	1.60	0.89	1.31	2.10
497	2.47	1.38	2.03	1.27
263.99	1.52	0.87	1.24	2.87
358.99	2.10	1.20	1.72	1.16
361.07	1.79	0.87	1.23	1.73
530.34	2.60	1.26	1.79	1.14
334.39	2.01	0.95	1.33	2.58
422.62	2.51	1.19	1.66	1.15
418.78	1.40	0.78	1.20	1.89
473.98	1.59	0.89	1.36	1.00
367.99	1.40	0.79	1.20	2.57
508.96	1.95	1.11	1.67	1.30
478	1.61	0.93	1.36	1.72
620.98	2.05	1.18	1.74	1.18
453.96	1.72	1.01	1.46	2.27
491.97	1.89	1.11	1.60	1.12
514.98	1.53	0.73	1.23	1.07
1025.97	3.11	1.48	2.50	1.47
470	1.77	0.87	1.40	1.16
799.97	3.03	1.48	2.39	1.28
591.13	1.79	0.78	1.28	1.10
863.85	2.57	1.12	1.85	1.14
547.53	2.11	0.92	1.45	1.22
784.75	3.05	1.32	2.09	1.17
637.98	1.34	0.64	1.12	0.98
1036.92	2.14	1.03	1.80	1.16
590.97	1.44	0.71	1.20	1.00
960.98	2.37	1.16	1.98	1.18
773.97	1.60	0.78	1.33	1.07
1180	2.41	1.18	2.02	1.24
705.07	1.69	0.84	1.40	1.10
986.99	2.47	1.24	2.05	1.16
Avg	2.02	1.62	1.59	1.15
Std	0.50	0.43	0.36	0.21

empirical methods (see Table 5). The best performance by values of  $N_u$  in columns of CFDST in this study is shown by average value 1.01 and 0.15 standard deviation of  $N_{u,Exp}/N_{u,Present\ study}$ . Overall, the results illustrated that the proposed MLR model in simulation and prediction of ultimate axial strength of CFDST columns

with active confinement is most reliable compared with those empirical equations.

## 5. CONCLUSION

The construction and design of formidable and massive engineering structures has been increasing in recent decades. These sturdy structures are designed for various aims, have a longer service life, and are needed for worldwide sustainable solutions. Thus, the cost optimization could be done through composite structures, and also the concerns mitigate because they couple the materials favorable engineering properties. In this line, CFDST members can enhance composite construction efficiency potentially. Nevertheless, delving these members into the main aspects is through the compression characteristics assessment of each cross-section element to provide reliable design guidelines. The test program in this study has sixty-four composite columns. In order to anticipate the performance of variables and characterize the internal and external steel tubes in the columns of CFDST, four various ratios of  $D_o/t_o$ , two ratios of  $D_i/t_i$ , and two distinct grades of strength were used. In this regard, the stress against the curves of strain and modes of failure subject to passive and active confinement were examined. Moreover, the application of the proposed design CFDST columns formula in the present study was evaluated through three prediction procedures of design capacity compared to the experimental results. The following conclusions can be considered in the scope of this study:

- The capacity of the load-carrying of specimens of CFDST can be noticeably enhanced by converting the type of confinement to active using this technique. The improvement ratio between the actively-confined and passively-confined CFDST differs from 1.25 to 1.75.

- The capacity of the circular columns load-carrying can improve effectively by the increase and decrease of concrete strength and steel tube  $D_o/t_o$ , respectively .

- Since the ratio of tube  $D_i/t_i$  enhances, the capacity of the CFDST loading capacity for the values of permanent  $D_o/t_o$  in the active confinement could not increase specifically when the tube thickness or inner diameter decrease .

- The provided capacity method of Uenaka in double skin columns capacity prediction performs very well. However, it is noteworthy that the formulation of this method is for CFDST columns of non-prestressed and does not consider the condition of active confinement .

- The predictions of the proposed formula are in line with the empirical results compared to the current formulas of strength prediction. They can predict the strength of the circular short CFDST columns compressive reasonably in the existence of active and passive confinement.

## 6. REFERENCES

- Han, L.-H., Li, W. and Bjorhovde, R., "Developments and advanced applications of concrete-filled steel tubular (cfst) structures: Members", *Journal of constructional steel research*, Vol. 100, (2014), 211-228, doi: 10.1016/j.jcsr.2014.04.016.
- Essopjee, Y. and Dundu, M., "Performance of concrete-filled double-skin circular tubes in compression", *Composite Structures*, Vol. 133, (2015), 1276-1283, doi: 10.1016/j.compstruct.2015.08.033.
- Borzouyi Kutenayi, S., Kiahosseini, S. and Talebpour, M., "The effect of caspian sea water on corrosion resistance and compressive strength of reinforced concrete containing different sio<sub>2</sub> pozzolan", *International Journal of Engineering, Transactions A: Basics*, Vol. 30, No. 10, (2017), 1464-1470, doi: 10.5829/ije.2017.30.10a.06.
- Wang, Y., Chen, G., Wan, B., Han, B. and Ran, J., "Axial compressive behavior and confinement mechanism of circular frp-steel tubed concrete stub columns", *Composite Structures*, Vol. 256, (2021), 113082, doi: 10.1016/j.compstruct.2020.113082.
- Hemmati, A. and Mojaddad, S., "Effect of steel confinement on behavior of reinforced concrete frame", *Journal of Rehabilitation in Civil Engineering*, Vol. 7, No. 3, (2019), 1-14, doi: 10.22075/jrce.2018.13791.1252.
- Seyed Razzaghi, M., Esfandyari, R. and Nateghi, F., "The effects of internal and external stiffeners on hysteretic behavior of steel beam to cft column connections", *International Journal of Engineering, Transactions A: Basics*, Vol. 27, No. 7, (2014), 1005-1014, doi: 10.5829/idosi.ije.2014.27.07a.01.
- Cheng, B. and Su, R., "Numerical studies of deep concrete coupling beams retrofitted with a laterally restrained steel plate", *Advances in Structural Engineering*, Vol. 14, No. 5, (2011), 903-915, doi: 10.1260/1369-4332.14.5.903.
- Zhao, X.-L., Tong, L.-W. and Wang, X.-Y., "Cfdst stub columns subjected to large deformation axial loading", *Engineering Structures*, Vol. 32, No. 3, (2010), 692-703, doi: 10.1016/j.engstruct.2009.11.015.
- Young, B. and Ellobody, E., "Experimental investigation of concrete-filled cold-formed high strength stainless steel tube columns", *Journal of Constructional Steel Research*, Vol. 62, No. 5, (2006), 484-492, doi: 10.1016/j.jcsr.2005.08.004.
- Kodur, V. and MacKinnon, D., "Simplified design of concrete-filled hollow structural steel columns for fire endurance", *Journal of Constructional Steel Research*, Vol. 1, No. 46, (1998), 298, doi: 10.1016/s0143-974x(98)80034-5.
- Zhu, A.-Z., Xu, W., Gao, K., Ge, H.-B. and Zhu, J.-H., "Lateral impact response of rectangular hollow and partially concrete-filled steel tubular columns", *Thin-Walled Structures*, Vol. 130, (2018), 114-131, doi: 10.1016/j.tws.2018.05.009.
- Mohammed, A.H., Mohammedali, T.K. and Hussin, A.K., "Experimental study on performance of fiber concrete-filled tube columns under axial loading", *International Journal of Engineering, Transactions C: Aspects*, Vol. 32, No. 12, (2019), 1726-1732, doi: 10.5829/ije.2019.32.12c.05.
- Wang, W.-D., Jia, Z.-L., Shi, Y.-L. and Tan, E.L., "Performance of steel-reinforced circular concrete-filled steel tubular members under combined compression and torsion", *Journal of Constructional Steel Research*, Vol. 173, (2020), 106271, doi: 10.1016/j.jcsr.2020.106271.
- Thai, S., Thai, H.-T., Uy, B. and Ngo, T., "Concrete-filled steel tubular columns: Test database, design and calibration", *Journal of Constructional Steel Research*, Vol. 157, (2019), 161-181, doi: 10.1016/j.jcsr.2019.02.024.
- Wei, Y., Jiang, C. and Wu, Y.-F., "Confinement effectiveness of circular concrete-filled steel tubular columns under axial compression", *Journal of Constructional Steel Research*, Vol. 158, (2019), 15-27, doi: 10.1016/j.jcsr.2019.03.012.
- Liu, X., Xu, C., Liu, J. and Yang, Y., "Research on special-shaped concrete-filled steel tubular columns under axial compression", *Journal of Constructional Steel Research*, Vol. 147, (2018), 203-223, doi: 10.1016/j.jcsr.2018.04.014.
- Jin, L., Fan, L., Li, P. and Du, X., "Size effect of axial-loaded concrete-filled steel tubular columns with different confinement coefficients", *Engineering Structures*, Vol. 198, (2019), 109503, doi: 10.1016/j.engstruct.2019.109503.
- Yuan, F., Huang, H. and Chen, M., "Effect of stiffeners on the eccentric compression behaviour of square concrete-filled steel tubular columns", *Thin-Walled Structures*, Vol. 135, (2019), 196-209, doi: 10.1016/j.tws.2018.11.015.
- Rahmani, Z., Naghipour, M. and Nematzadeh, M., "Flexural performance of high-strength prestressed concrete-encased concrete-filled steel tube sections", *International Journal of Engineering, Transactions C: Aspects*, Vol. 32, No. 9, (2019), 1238-1247, doi: 10.5829/ije.2019.32.09c.03.
- Jiang, Y., Silva, A., Macedo, L., Castro, J.M., Monteiro, R. and Chan, T.-M., "Concentrated-plasticity modelling of circular concrete-filled steel tubular members under flexure", in *Structures*, Elsevier. Vol. 21, (2019), 156-166.
- Al Zand, A.W., Badaruzzaman, W.H.W., Mutalib, A.A. and Hilo, S.J., "Flexural behavior of cfst beams partially strengthened with unidirectional cfrp sheets: Experimental and theoretical study", *Journal of Composites for Construction*, Vol. 22, No. 4, (2018), 04018018, doi: 10.1061/(asce)cc.1943-5614.0000852.
- Ho, J. and Dong, C., "Improving strength, stiffness and ductility of cfdst columns by external confinement", *Thin-Walled Structures*, Vol. 75, (2014), 18-29, doi: 10.1016/j.tws.2013.10.009.
- Wei, S., Mau, S., Vipulanandan, C. and Mantrala, S., "Performance of new sandwich tube under axial loading: Experiment", *Journal of Structural Engineering*, Vol. 121, No. 12, (1995), 1806-1814, doi: 10.1061/(asce)0733-9445(1995)121:12(1806).
- Han, L.-H., Huang, H., Tao, Z. and Zhao, X.-L., "Concrete-filled double skin steel tubular (CFDST) beam-columns subjected to cyclic bending", *Engineering Structures*, Vol. 28, No. 12, (2006), 1698-1714, doi: 10.1016/j.engstruct.2006.03.004.
- Yagishita, F., Kitoh, H., Sugimoto, M., Tanihira, T. and Sonoda, K., "Double skin composite tubular columns subjected to cyclic horizontal force and constant axial force", in *Proc., 6th ASCCS Int. Conf. on Steel-Concrete Composite Structures*, Univ. of Southern California Los Angeles. (2000), 497-503.
- Li, W., Ren, Q.-X., Han, L.-H. and Zhao, X.-L., "Behaviour of tapered concrete-filled double skin steel tubular (CFDST) stub columns", *Thin-Walled Structures*, Vol. 57, (2012), 37-48, doi: 10.1016/j.tws.2012.03.019.
- Nematzadeh, M., Hajirasouliha, I., Haghinejad, A. and Naghipour, M., "Compressive behaviour of circular steel tube-confined concrete stub columns with active and passive confinement", *Steel Composite Structures, An International Journal*, Vol. 24, No. 3, (2017), 323-337, doi: 10.1016/j.engstruct.2016.10.008.
- Nematzadeh, M., Naghipour, M., Jalali, J. and Salari, A., "Experimental study and calculation of confinement relationships for prestressed steel tube-confined compressed concrete stub columns", *Journal of Civil Engineering Management*, Vol. 23, No. 6, (2017), 699-711, doi: 10.3846/13923730.2017.1281837.
- Nematzadeh, M., Fazli, S., Naghipour, M. and Jalali, J., "Experimental study on modulus of elasticity of steel tube-confined concrete stub columns with active and passive

- confinement", *Engineering Structures*, Vol. 130, (2017), 142-153, doi: 10.1016/j.engstruct.2016.10.008.
30. Testing, A.S.f., Materials. Committee A-01 on Steel, S.S. and Alloys, R., "Standard test methods and definitions for mechanical testing of steel products, ASTM International, (2017).
  31. Concrete, A.I.C.C.o. and Aggregates, C., "Standard test method for compressive strength of cylindrical concrete specimens, ASTM international, (2014).
  32. Committee, A., "Building code requirements for structural concrete: (aci 318-02) and commentary (aci 318r-02), American Concrete Institute. (2002).
  33. Uenaka, K., Kitoh, H. and Sonoda, K., "Concrete filled double skin circular stub columns under compression", *Thin-Walled Structures*, Vol. 48, No. 1, (2010), 19-24, doi: 10.1016/j.tws.2009.08.001.
  34. AII, *Standard for structural calculation of steel reinforced concrete structures*. 2001.
  35. Hassanein, M., Kharoob, O. and Liang, Q., "Circular concrete-filled double skin tubular short columns with external stainless steel tubes under axial compression", *Thin-Walled Structures*, Vol. 73, (2013), 252-263, doi: 10.1016/j.tws.2013.08.017.
  36. Liang, Q.Q. and Fragomeni, S., "Nonlinear analysis of circular concrete-filled steel tubular short columns under axial loading", *Journal of Constructional Steel Research*, Vol. 65, No. 12, (2009), 2186-2196, doi: 10.1016/j.jcsr.2009.06.015.
  37. Liang, Q.Q., "Performance-based analysis of concrete-filled steel tubular beam-columns, part i: Theory and algorithms", *Journal of Constructional Steel Research*, Vol. 65, No. 2, (2009), 363-372, doi: 10.1016/j.jcsr.2008.03.007.

---

### Persian Abstract

---

#### چکیده

یکی از عضوهای رایج و در دسترس ستون‌های کامپوزیتی، لوله دو جداره پر شده از بتن (CFDST) است. این ستونها شامل دو لوله از فولاد متحدالمرکز و همچنین بتنی است که بین آنها وجود دارد. مشخصه‌های مکانیکی ستون‌های CFDST بیشتر از نمونه‌های مشابه با لوله‌های یک جداره فولادی پر شده از بتن (CFST) است. هدف از مطالعه حاضر ارائه نتایج تحقیقات آزمایشگاهی در مورد ظرفیت باربری ستون‌های CFDST با پیش‌تندگی فعال است. در اینجا، یک تکنیک ابتکاری برای پیش‌تندگی بتن محصور شده استفاده می‌شود که در آن بتن تازه برای مدت کوتاهی فشرده می‌شود. در مجموع شصت و چهار نمونه با ضخامت‌ها و قطرهای بیرونی و داخلی مختلف و همچنین ستون‌های CFDST با مشخصه‌های مختلف بتن، آزمایش شدند. نتایج آزمایشگاهی نشان می‌دهد که روش به کارگرفته شده برای بتن محصور شده ظرفیت باربری نمونه‌های CFDST را به طور قابل توجهی افزایش می‌دهد.

---